

Analysis of the XMM-Newton EPIC Background: Production of Background Maps and Event Files

Andrew M. Read

School of Physics & Astronomy, University of Birmingham,
Birmingham B15 2TT, UK

amr@star.sr.bham.ac.uk <http://www.sr.bham.ac.uk/~amr>

<http://www.sr.bham.ac.uk/xmm3/>

Abstract

XMM-Newton background maps for the 3 EPIC instruments in their different instrument/mode/filter combinations and in several energy bands have been constructed using a superposition of many pointed observations. Event datasets for the different instrument/mode/filter combinations have also been constructed, with longer exposure times than previously created files. This document describes the construction of the background maps and event files, and their usage. Further details on how to obtain these background products, together with related software and these explanatory notes can be found at <http://www.sr.bham.ac.uk/xmm3/BGproducts.html>.

1 Introduction

The XMM-Newton observatory provides unrivalled capabilities for detecting low surface brightness emission features from extended and diffuse galactic and extragalactic sources, by virtue of the large field of view of the X-ray telescopes with the EPIC MOS (Turner et al. 2001) and pn (Strüder et al. 2001) cameras at the foci, and the high throughput yielded by the heavily nested telescope mirrors. The satellite has the largest collecting area of any imaging X-ray telescope.

In order to exploit the excellent EPIC data from extended objects, the EPIC background, known now to be higher than estimated pre-launch, needs to be understood thoroughly. With a good model of the particle and photon background, one can correctly background-subtract images and spectra extracted over different energy bands and from different areas of the detectors.

The initial aim of the project described here had been to make use of slew data to help define the EPIC background and vignetting. As no significant amount of useful slew data has so far been acquired, it was decided to use a large number of XMM-Newton pointed observations to produce background maps for each of the three EPIC instruments (pn, MOS1 & MOS2) and in several different energy bands. Also, significantly improved background event files, extremely useful in terms of spectral analysis, with longer exposures than previously produced files, and specific to several particular instrument/mode/filter combinations, have been created as a by-product of the analysis. The adding together of many fields allows the minimization of any ‘cosmic variance’, resulting from variations in the local diffuse X-ray emission or contamination from pathologically bright sources.

This document is intended as an aid when using these files. The current understanding of the XMM-Newton background is described briefly in Section 2. Section 3 describes the methods used in the creation of the background products. Information regarding how to use the background images for XMM EPIC background analysis can be found in Section 4, along with caveats as to their use. The relevant information for the event files can be found in Section 5.

All the background product files (maps, event files, related software etc.) are available together with this document, and other scripts and procedures to do with XMM-Newton Background Analysis on <http://www.sr.bham.ac.uk/xmm3/>

2 The XMM-Newton X-ray Background

The EPIC background has been shown (via the work of Lumb et al. (2002) and many others; see Appendix) to mainly comprise:

- Solar soft protons (see Sect.3.2) perhaps accelerated by ‘magnetospheric reconnection’ events, and gathered by XMM-Newton’s grazing mirrors (and perhaps trapped beforehand by the Earth’s magnetosphere). These dominate the times of high background. During quiescent periods (i.e. with no significant soft proton contamination), the remaining components are:
- High energy, non-vignetted cosmic ray induced events, unrejected by the the on-board electronics. Also, associated instrumental fluorescence, due to the interaction of high-energy particles with the detector.
- Non-vignetted electronic noise i.e. bad (bright) pixels (and dark current, though this may be negligible).
- Low to medium energy, vignetted X-ray photons from the sky. This can be divided into the local (predominately soft) X-ray background, the cosmic (harder) X-ray background, and single reflections entering the telescope from bright sources outside of the nominal field of view (FOV). Lumb et al. (2002) estimate that the contribution of diffuse flux gathered from out-of-field angles of 0.4–1.4 degrees is of order 7% of the true, focussed in-field signal, and the associated systematic error (due mainly to the energy dependence) is $\pm 2\%$.

Table 1 gives a very brief summary of the temporal, spatial and spectral properties of these, the major components contributing to the XMM-Newton background.

The present analysis is related in several respects to the work of Lumb et al. (2002), and the reader is encouraged to consult this work. Additional notes regarding other related work on the EPIC background can be found in the Appendix.

3 Analysis

Source-subtracted, high-background-screened and exposure- and source-corrected images (maps) of the particle and photon components of the EPIC background have been created separately for each EPIC instrument, and in several different energy bands. This has been performed separately per observation, over a large number of individual observations.

The individual background maps for a particular instrument and in a particular energy band have then then been collected together (for the same instrument mode/filter combination) over the whole set of observations. Via various cleaning, filtering and ‘ σ -clipping’ techniques, a ‘mean’ background map is created (for each particular background component/instrument/energy band/mode/filter combination).

Procedures have been written to perform the different aspects of the analysis, making extensive use of the XMM-SAS tasks, some Chandra CIAO tools and HEASOFT’s FTOOLS utilities.

Before discussing the analysis in depth, it is worth describing some of the files and terms used, and defining the structure of some of the final products.

3.1 Analysis: Files & Definitions

Here are defined a number of terms used in the following description of the analysis, and of the product files and maps, and their usage.

- Background maps. Detector maps of all the background components combined i.e. soft and hard X-ray photons (vignetted), internal particles (non-vignetted), some small factor of soft protons (scattered/funelled) and single-reflections from out-of-FOV sources.
- Vignetting maps. Detector maps of the effective area i.e. the above background maps minus the particle and single-reflection contributions.
- Detector maps. Images in detector coordinates (DETX DETY) (as opposed to sky coordinates), defined in the present analysis such that the individual pixels are $1'$ by $1'$, DETX/DETY of (0,0) lies at a pixel intersection, and the full area of the CCDs is covered. More detailed information

Table 1: Summary of the components within the XMM-Newton Background; temporal, spatial and spectral properties

	PARTICLES			PHOTONS	
	SOFT PROTONS	INTERNAL (Cosmic-ray induced)	ELECTRONIC NOISE	HARD X-RAYS	SOFT X-RAYS
Source	Few 100 keV solar protons	Interaction of High Energy particles with detector	1) Bright pixels 2) Electronic overshoot near pn readout	X-ray background (AGN etc)	Local Bubble Galactic Disk Galactic Halo
Variable? (per Obs) (Obs to Obs)	Flares (>1000%) Unpredictable. More far from apogee. Low-E flares turn on before high-E	$\pm 10\%$ $\pm 10\%$ No increase after solar flares	$\pm 10\%$ 1) >1000% (pixels come and go, also meteor damage)	Constant Constant	Constant Variation with RA/Dec ($\pm 35\%$)
Spatial Vignetted? Structure?	Yes (scattered) Perhaps, unpredictable	No Yes. Detector + construction MOS: outer 6 CCDs more Al, CCD edges more Si PN: Central hole in high-E lines (~ 8 keV)	No Yes 1) Individual pixels & columns 2) Near pn readout (CAMEX)	Yes No	Yes No, apart from real astronom. objects
Spectral	Variable Unpredictable No correlation between intensity + shape Low-E flares turn on before high-E	Flat + fluorescence + detector noise MOS: 1.5 keV Al-K 1.7 keV Si-K det.noise<0.5 keV. High-E – low-intensity lines (Cr, Mn, Fe-K, Au) PN: 1.5 keV Al-K no Si (self-absorbed) Cu-Ni-Zn-K (~ 8 keV) det.noise<0.3 keV	1) low-E (<300 eV), tail may reach higher-E 2) low-E (<300 eV)	~ 1.4 power law. Above 5keV, dominates over internal component	Thermal with $\lesssim 1$ keV emission lines

Table 2: Detailed information as to the coordinate systems of the 1' background detector maps and the 4'' detector maps used within the analysis.

Instrument	Coord. (DETX/Y)	Range in		Number of pixels in maps					
		Detector coords.		Small-scale (4'')			Large-scale (1')		
		min.	max.	N _{-ve}	N _{+ve}	N _{tot}	N _{-ve}	N _{+ve}	N _{tot}
PN	DETX	-19199	14400	240	180	420	16	12	28
	DETY	-16799	15600	210	195	405	14	13	27
M1	DETX	-20399	20400	255	255	510	17	17	34
	DETY	-20399	20400	255	255	510	17	17	34
M2	DETX	-20399	20400	255	255	510	17	17	34
	DETY	-20399	20400	255	255	510	17	17	34

as to the coordinate system used (and of the 4'' detector maps used within the analysis) is given in Table 2. Software has been written (see Sect. 4.2) to rebin the detector maps to any spatial scale, and to reproject the maps to any sky coordinates (given via a user-input sky image).

- **Instruments.** The present analysis has been performed for each of the EPIC instruments; pn, MOS1 & MOS2 (hereafter PN, M1, M2).
- **Instrument mode & filter.** Several different data acquisition modes exist for each of the EPIC instruments. Also, observations have been taken using different filters for each of the EPIC instruments. The present analysis has been performed for the most common instrument mode/filter combinations, and those most useful to the analysis of diffuse X-ray emission from extended objects. These are full-frame mode with thin filter (ft) and full-frame mode with medium filter (fm), for each of PN, M1 & M2, and also (for PN) full-frame-extended mode with thin filter (et) and full-frame-extended mode with medium filter (em).
- **Energy bands.** The analysis has been performed in the following XMM-XID & PPS standard energy bands; energy bands 1–5, defined as follows; 1: 200–500 eV 2: 500–2000 eV 3: 2000–4500 eV 4: 4500–7500 eV 5: 7500–12000 eV, and the full energy band 0: 200–12000 eV.
- **Closed datasets.** A few XMM observations have been obtained with the filter wheel in the ‘closed’ position. No photons reach the CCDs, so the event files contain only the instrumental and particle components of the background. Such datasets have been collected together and processed, and exist on <ftp://www-station.ias.u-psud.fr/pub/epic/Closed> (Marty 2002). They are dependent on the instrumental mode, and have been processed for M1 full-frame, M2 full-frame, PN full-frame and PN full-frame-extended mode.

3.2 Analysis: Data Preparation and Reduction

The initial analysis is essentially the same for each observation.

- For each observation, the relevant Pipeline Processing System (PPS) products (event lists, source lists, attitude files, housekeeping files etc.), from the standard analysis carried out at the SSC, are collected together.
- For each instrument, region files are created from the PPS source lists. These are then used to remove all the source events from each of the relevant event files. A conservative extraction radius of 36'' is used to remove the sources (for comparison, Lumb et al. (2002) used 25''). All the sources are also removed from previously created mask files (these are required to calculate losses in area due to source removal).
- A visual inspection is made of the data to make sure that there are no strange features in the field, and to ascertain whether there are any very bright point sources or large diffuse sources which could contaminate the background, even after source subtraction.

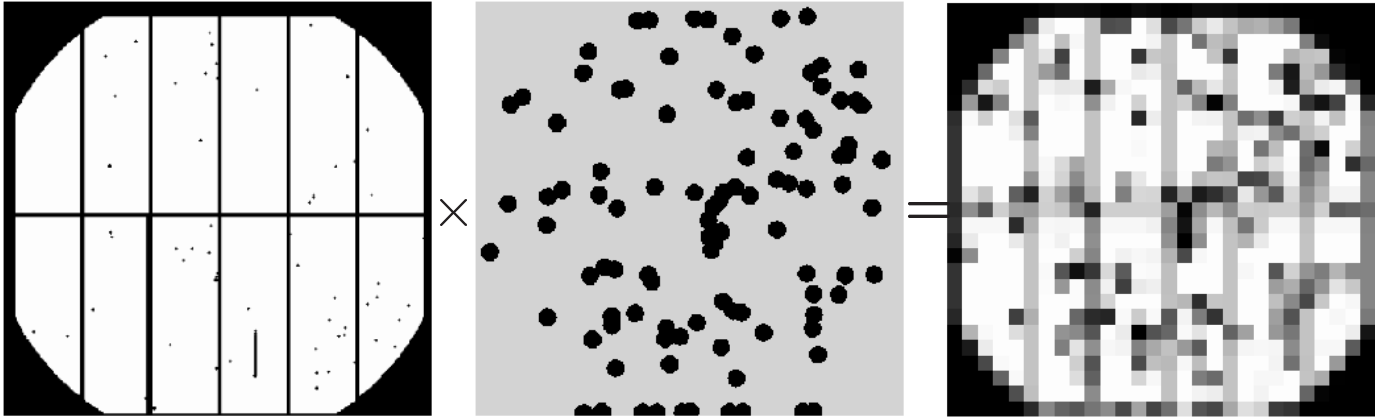


Figure 1: A non-vignetted ($4''$) exposure map is multiplied by a source-removed ($4''$) mask map and rebinned to create a large-scale ($1'$) ‘area-times-exposure’ map (example is for PN).

- Each of the event files are then filtered for periods of high background (solar proton flares). Lightcurves are created over the whole detector for single events in the energy range 10–15 keV and with FLAG values as defined by #XMMEA_EM or #XMMEA_EP. i.e. with the following expression for the XMM-SAS task evselect (e.g. for PN);

```
PI in [10000:15000] && #XMMEA_EP && PATTERN==0
```

Good Time Interval (GTI) files are created from these lightcurves on the basis of when the count rate falls below 100 (PN) or 35 (M1/M2) ct/100 s. The event files are then filtered, keeping the low count rate time periods.

- The event files are then filtered further. Events with energies below 150 eV are discarded. For PN, only singles and doubles are retained, for M1/M2, singles, doubles, triples and quadruples are retained. Finally, the event lists are filtered using the #XMMEA_EM/P FLAG expressions, excepting that events from outside the field of view (out-of-FOV) are kept.
- In the case of PN, it was necessary to further filter the files as regards a small number of persistent bad (bright) pixels/columns, occurring in many (though not all) of the observations. The same pixels were also found to contaminate the PN closed datasets. These pixels were removed from all the PN datasets. Given the large-scale ($1'$) of the final BG maps, this made a very small difference, as the loss in area is very small. Nevertheless, this difference was corrected for in the final maps. The pixels removed were as follows: CCD1 col.13 & (56,75), CCD2 (46–47,69–72), CCD5 col.11, CCD7 col.34, CCD10 col.61, CCD11 (47–48,153–156) (50,161–164). No bad pixels were removed from any of the MOS datasets (pointed observations or closed datasets). The event files are now filtered and have had all sources removed.
- For each of the three instruments, a small-scale ($4''$) non-vignetted exposure map (with dimensions as given in Table 2) is created. From the source-removed mask file, an area map ($4''$) is created, containing zero values at the positions where sources have been removed, and unity values elsewhere. These two maps are combined and rebinned to form a large-scale ($1'$; see Table 2) ‘area-times-exposure’ map (see Fig.1).
- For each instrument (of 3) and each energy range (of 6), ($1'$) detector maps are created. Because X-ray photons cannot reach the out-of-FOV areas of the detector, the events in these areas of the detector are solely due to the instrumental and particle components of the background. By making use of the Closed datasets, and comparing the number of counts in the out-of-FOV regions of the Closed datasets and the particular observation dataset in question, one can separate (for each mode-dependent instrument and energy range) the ($1'$) detector map into a particle (pa) map, containing the particle and instrumental background components and a photon (ph) map, containing the photon component of the background. This is done, producing 2 maps for each instrument and each energy range.

- The particle images are then exposure-corrected via a direct division by the LIVETIME (corrected for periods of high background and deadtime, deadtime being times when detector areas are affected by cosmic rays, and therefore not available to detect valid X-rays), and a division by a $1'$ detector mask of the sensitive area of the CCDs (to correct for chip gaps). The photon images are exposure-corrected via a division by the appropriate ‘area-times-exposure’ map.

3.3 Analysis: Observation, Mode and Filter Selection

The above preparational analysis has been performed for a large number of XMM-Newton observations, spanning a large range in instrumental modes used, filters used, exposure times and degree and duration of high-background flaring.

In order to produce the final background maps, the observations have been collected together in terms of the above requirements. Further, all observations containing a significantly bright source whose wings could still contaminate the background after source subtraction have been removed from the subsequent analysis. Similarly, all observations containing a large diffuse source, which could contribute to the estimated background, have been removed. All observations where the background flaring was of such an extent that, after flare-removal, less than 10% of the original exposure remained, were also removed.

The remaining 72 ‘clean’ observations used in the production of the final background files are summarized in Table 3, which lists the revolution number, the source target name, and a code giving the instrumental mode and filter for, respectively, M1, M2 and PN [f - full-frame mode, e - full-frame-extended mode, t - thin filter, m - medium filter]. Also given are the nominal exposure time, and the fraction of the exposure time remaining after removal of high-background periods and accounting for deadtime effects.

Table 4 summarizes the final cleaned observation information in terms of the different combinations of instrument, instrument mode and filter used. The exposure time is the sum of the individual LIVETIMES i.e. corrected for periods of high-background and deadtime.

3.4 Analysis: Cubes and Clipping

The basic principle involved in the production of a single ‘averaged’ background map from many background maps over different observations is that of removing the outliers which may represent images that are contaminated at a particular pixel.

In order to produce a particular set of background maps (in the different energy bands) for a particular instrument/mode/filter combination, the following steps are taken. Let us take for example the first entry in table 4, i.e. MOS1, full-frame mode, thin filter.

For each of the 49 relevant observations, comprising in total over 1 Msec of clean, low-background data, the 0-band (full energy band) $1'$ photon detector maps of the background are stacked together into a 3-D ‘imagecube’ (see Fig. 2) of dimensions DETX, DETY (each in the case of MOS1 of size 34; see Table 2) and N_{obs} (of size, in this example, 49).

For each DETX/DETY, a statistical analysis of the (in this case, 49) values at that particular DETX/DETY point is performed. Here, a ‘clipcube’ is constructed (of dimensions identical to the input imagecube), containing information (1’s and 0’s) as to which cells in the imagecube are within the allowed range and which values are not, i.e. which values are ‘clipped’ (see Fig. 3). The allowable range is defined as within some number of standard deviations (σ) from the mean value at that DETX/DETY. For the present analysis, this number of σ s is set at 1.2. Several steps are taken to ensure that the initial mean used to define the clip limits is not seriously biased by outliers. The mean value at that particular DETX/DETY is then calculated from the remaining ‘ σ -clipped’ values.

Imagecubes are then created, as in the 0-band, from the intermediate energy band (bands 1–5) $1'$ photon detector maps of the background. A σ -clipped image is then created from these cubes, but using the previously created relevant 0-band clipcube to remove values from each (band 1–5) imagecube. The same procedure is performed for the particle images, and for all instrument/mode/filter combinations.

Table 3: Summary of the cleaned and filtered observations used in the production of the EPIC background files. Given is the revolution number, the source target name, and a code giving the instrumental mode and filter for M1, M2 and PN [f - full-frame mode, e - full-frame-extended mode, t - thin filter, m - medium filter]. Also given is the nominal exposure time, and the fraction of the exposure time remaining after removal of high-background periods.

Rev.	Source	Mode/Filter (M1M2PN)	Expos. (s)	f(Exp.)	Rev.	Source	Mode/Filter (M1M2PN)	Expos. (s)	f(Exp.)
281	MS1054.4-0321	ft ft et	40260	0.61	324	PMN0525-3343	ft ft ft	27786	0.65
283	IC1623	fmfmfm	11813	0.13	339	NGC2563	fmfmfm	21617	0.88
284	C2001	ft ft ft	9900	0.40	343	S308	fmfmem	47559	0.37
285	ESO263-6048	fmfmem	9215	0.89	344	IRAS07598+6508	fmfmfm	22615	0.73
286	NGP rift1	ft fmet	24211	0.81	345	SC223	fmfmem	34326	0.45
286	NGP rift2	ft fmet	24211	0.89	345	3C192	ft ft et	24326	0.70
286	NGP rift3	ft fmet	24214	0.66	346	3EG0616-3310	ft ft et	11773	0.90
287	XMDSOM 5	ft ft et	24218	0.89	346	3EG0616-3310	ft ft et	14772	0.46
287	XMDS SSC 3	ft ft et	24318	0.89	346	3EG0616-3310	ft ft et	14771	0.71
287	XMDS SSC 4	ft ft et	28512	0.88	346	APM08279+5255	fmfmfm	16916	0.90
287	XMDS SSC 5	ft ft et	24313	0.87	347	CEGru	ft ft ft	7615	0.91
288	1saxj2331.9+1938	fmfmfm	11513	0.77	348	NGC3184	ft ft ft	29617	0.76
288	XMDS SSC 1	ft ft et	25149	0.74	348	RXJ0911.4+0551	ft ft et	20072	0.22
288	XMDS SSC 2	ft ft et	12268	0.17	349	Lockman Hole	fmfmfm	37950	0.77
288	SGP-3	ft ft et	9209	0.62	353	Arp270	ft ft et	37800	0.36
299	AXAF Ultra Deep	ft ft et	39765	0.49	353	RXJ1011.2+5545	xx ft ft	32615	0.83
299	AXAF Ultra Deep	ft ft et	56698	0.65	353	UGC05101	fmfmet	34371	0.89
300	H1413+117	ft ft et	25719	0.88	354	NGC7252	fmfmfm	27617	0.85
305	ERO field	ft ft ft	40387	0.86	354	MS2053.7-0449	xx fmem	16770	0.89
307	Omega cen	fmfmfm	39978	0.47	355	LBQS2212-1759	ft ft xx	34397	0.96
308	XMDS SSC 2	ft ft et	12666	0.89	355	LBQS2212-1759	ft ft ft	10824	0.62
310	XTEJ0421+560	fmfmfm	32310	0.40	356	LBQS2212-1759	ft ft ft	109427	0.77
311	CenX-4	ft ft ft	52799	0.43	359	NGC3044	ft ft et	10020	0.39
312	RXJ0002+6246	fmfmfm	33000	0.49	360	SextansA	fmfmem	19130	0.21
312	S50014+813	fmfmfm	39337	0.35	360	PG1115+080	fmfmft	62616	0.78
314	NGC2146	fmfmft	26847	0.40	360	NGC4138	ft ft em	14317	0.87
316	GRS1716-249	ft ft ft	12225	0.70	361	Arp222	ft ft et	14369	0.86
316	GROJ1655-40	fmfmfm	39820	0.46	361	RXJ2237.0-1516	ft ft et	24370	0.78
317	CFHT-PL-12	ft ft ft	34335	0.31	362	PG2302+029	ft ft ft	12566	0.88
317	L1448-C	ft ft ft	32725	0.32	363	LSBC F568-6	ft ft et	14365	0.47
317	SHARC-2	ft ft et	48870	0.64	364	NGC4168	ft ft em	22867	0.86
321	oph pos1	ft ft et	20121	0.88	366	CSO755	ft ft ft	36926	0.72
321	oph pos2	ft fmet	18626	0.82	383	LSS 2	ft ft et	13382	0.85
322	VII Zw031	fmfmfm	31997	0.90	383	LSS 6	ft ft et	13382	0.44
323	KS1731-260	ft ft ft	24618	0.61	383	LSS 7	ft ft et	12380	0.87
323	KS1731-260	ft ft ft	25115	0.60	451	NGC4490	fmfmem	17521	0.85

Table 4: Summary of the cleaned and filtered observations used in the production of the EPIC background files, separated into the different combinations of instrument, instrument mode and filter used. The exposure time is the sum of the individual LIVETIMES i.e. corrected for periods of high-background and deadtime.

Instrument	Mode	Filter	Number of Observations	Exposure Time (s)
MOS1	Full-Frame	Thin	49	1055905
MOS1	Full-Frame	Medium	21	488422
MOS2	Full-Frame	Thin	46	1004709
MOS2	Full-Frame	Medium	26	592975
PN	Full-Frame	Thin	18	351549
PN	Full-Frame	Medium	12	188159
PN	Full-Frame-Extended	Thin	32	416739
PN	Full-Frame-Extended	Medium	8	82957

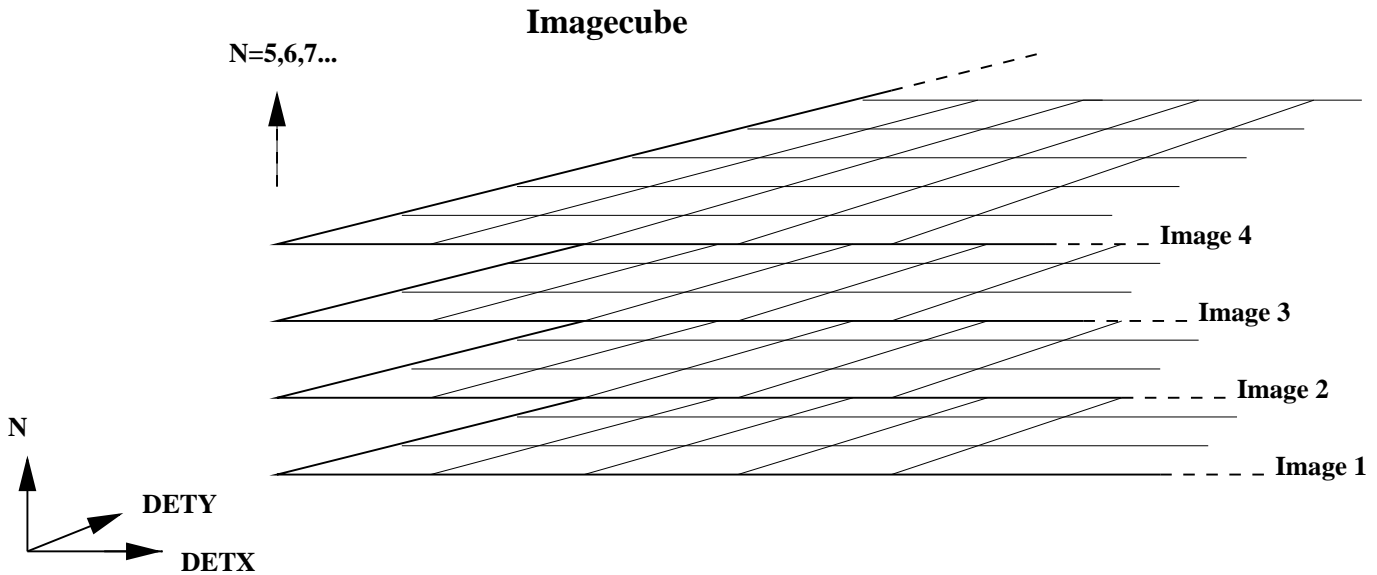


Figure 2: A 3-D 'imagecube' of dimensions $DETX$, $DETY$ and N_{obs} .

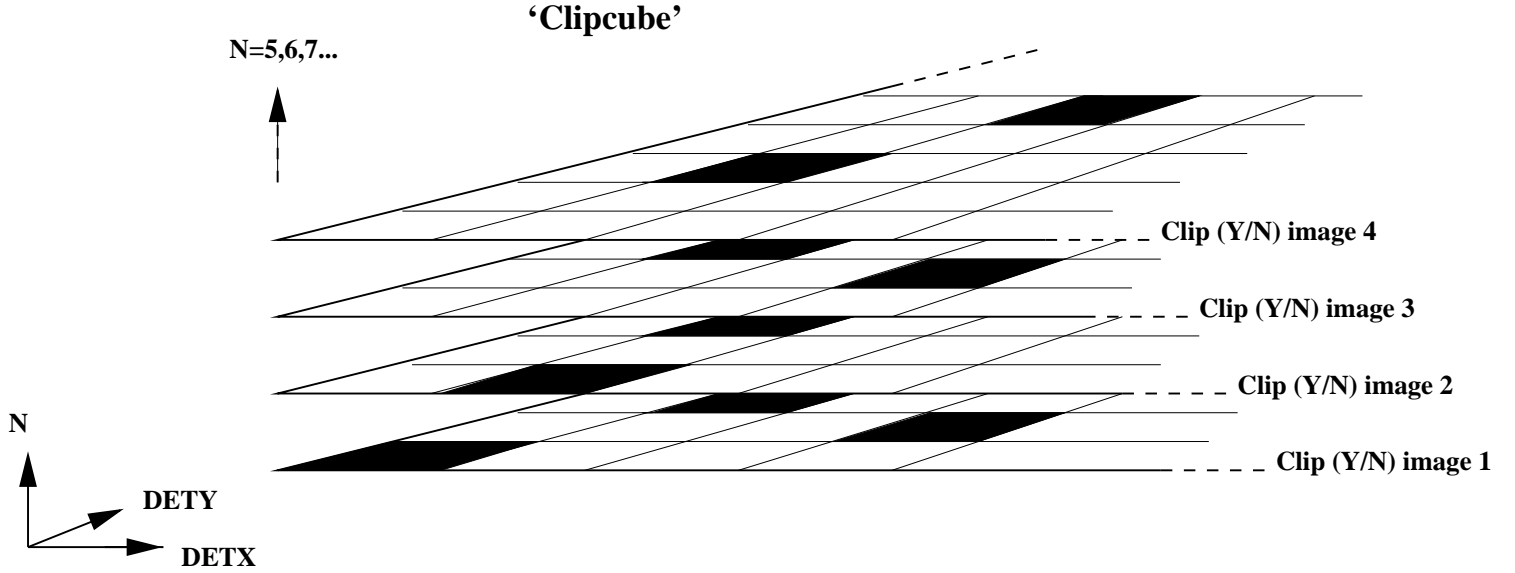


Figure 3: A 3-D ‘clipcube’ of dimensions DETX, DETY and N_{obs} . In this example, for DETX/DETY=(1,1), the value in image 1 is outside of the allowable range, and is to be clipped from the calculation of the mean value for DETX/DETY=(1,1).

4 The Background maps

σ -clipped, and averaged, exposure-corrected background maps have been created as described above for each instrument/mode/filter combination analysed (of 8) and in each energy band (of 6). Photon and particle maps have been created separately, as have maps with the two components recombined. This leads to a total of 144 background maps.

A1_ft0000_cphim4M1.fits is, as an example of the file naming, an exposure-corrected photon background map. A particle map has cpa_{im}, instead of cph_{im}, and a particle and photon combined map has cim. It is a MOS1 map (M1 instead of M2 or PN), and is in energy band 4 (of 0–6). The mode is full-frame (given by the f), as opposed to (for PN) extended full-frame mode (e), and the filter is thin (t), as opposed to medium (m). The six character mode+filter string is as in Table 3, hence the corresponding PN file has 0000ft.

4.1 The Background maps: Usage

How then can an observer with their own EPIC data make use of these background maps? In order to analyse extended objects, and make background-subtracted images, estimate low-surface brightness flux levels, create radial profiles or perform 1- or 2-D surface brightness fitting, one needs a map of the appropriate background. Sometimes however, the diffuse, extended nature of the user’s target source is such that the determination of the background from their own dataset is difficult or impossible. Also, using a background from a significantly removed section of the same data leads to problems with vignetting and detector variations. Hence the need for the independently-produced background maps created here.

What follows is a recipe for how an observer can make use of the background maps in conjunction with their own source data. Caveats, and problems that can occur when the recipe is not or can not be followed are given thereafter.

- The source data should be flare-rejected to a similar level to that performed in the creation of the background maps. ¹
- Source maps should be created from the flare-rejected source datasets in the same XID/PPS energy bands (bands 0–5) as used here. ²

- As a particular source map will be created (most commonly) in sky coordinates, and will have a resolution finer than $1'$, the routine *BGrebiniimage2SKY* should be used to rebin and sky-project the equivalent background map(s) to the resolution and sky position of the source map (see Sect. 4.2).
- Depending on whether the source maps are raw count maps or exposure-corrected flux maps, the equivalent rebinned background map(s) (which are exposure-corrected) may be scaled appropriately, either by an exposure time, or using an appropriate exposure map.
- A comparison of the counts or flux in the out-of-FOV areas of the source and background maps yields the scaling by which the particle component (the ‘cpaim’ map) of the background needs be scaled.³
- If source-free regions within the FOV exist within the source dataset, then count/flux comparisons in these regions yield the scaling for the photon component (the ‘cphim’ map). The scaled photon component can then be added to the scaled particle component to give the final background map.³

¹ If such a flare-rejection method as used here leads to zero or very few Good Times, then the user’s data is heavily flare-contaminated, and the background maps are therefore not suitable for source data extracted from the whole dataset. Small discrepancies due to slightly different flare-rejection methods may be accounted for by the subsequent scaling.

² Though the user should work using the same energy bands (bands 0–5) as used in the present analysis, note that the standard XID/PPS bands have been used, and that extension to larger energy bands can easily be performed by summing individual band images. For example, band 1 is heavily contaminated by detector noise in the particle background, so the user may prefer to work in band (2+3+4+5).

³ If source-free regions within the FOV do exist within the source dataset, then the user is advised to work as above with the particle and photon (‘cpaim’ & ‘cphim’) maps separately. The particle and photon scaling factors may be different (hence the fact that separate particle and photon background maps have been made available). If no source-free regions exist, the user may be forced to assume that the scalings are the same. Here, just the ‘cim’ images need be used. A script for comparing out-of-FOV counts (from event files), *compareoutofFOV*, is available on <http://www.sr.bham.ac.uk/xmm3/>. Note especially that at the very edges of the map FOVs, there are a few pixels with unusually large and small values. This is due to extremely small exposure values in the original observation maps amplifying the noise. These areas should be avoided when calculating scaling values.

Note also that comparisons of the in- and out-of-FOV source maps are useful in characterizing the low-energy flare contamination (e.g. de Luca & Molendi 2002).

4.2 The Background maps: Sky coordinates, Rebinning and Reprojecting

Usually, of course, the user will work in sky coordinates (RA & Dec), not detector coordinates, and to a much finer scale than $1'$. With that in mind, software has been developed to rebin and reproject onto the sky any provided background map (scaled or otherwise) to the spatial scale and sky position of a user-input image.

BGrebiniimage2SKY is a shell script plus fortran routine to convert the low-resolution DETX/DETY background maps into high-resolution sky (X/Y) images. The user gives a template image containing the attitude information, and an event file (ideally, the one used to create the template image file, though any may do, as it is just for general header purposes). A rebinned background map is produced with the same resolution and at the same sky position as the template image. The radius of the interpolation circle can be given (note that the background DETX/DETY maps are of $1'$ resolution, so an interpolation radius of this or slightly larger is recommended).

```
Use: BGrebiniimage2SKY image imtemplate evfile rinterp outimage
      image      - Input image (low-res DETX/DETY image)
      imtemplate - Template image file containing attitude info (high-res SKY image)
      evfile     - Event file, ideally the one used to create imtemplate
```

```
rinterp    - Interpolation radius [arcmin] (1 - 1.5)
outimage   - Output image (high-res SKY image)
e.g. BGrebinimage2SKY BGimage.fits myimage.fits evfile.fits 1.2 newBGimage.fits
```

An example of the task in use can be seen in Fig.4.

5 Event files

As a by-product of the analysis, for each observation, event files have been created, in the same manner as Lumb et al. (2002), filtered for times of high background and with all sources removed. The relevant event files have been merged together for each instrument/mode/filter combination (Tables 3 & 4), and eight separate event files have therefore been created (with exposure times given as in Table 4), each having an extension containing a calibrated event list in the same format as produced by the XMM-SAS. The event files have had sky coordinates assigned to them for a pointing on the sky of RA=0, Dec=0, PA=0. These event files (or indeed any) can be reprojected onto any point in the sky via e.g. *skycast* (see <http://www.sr.bham.ac.uk/xmm3/>).

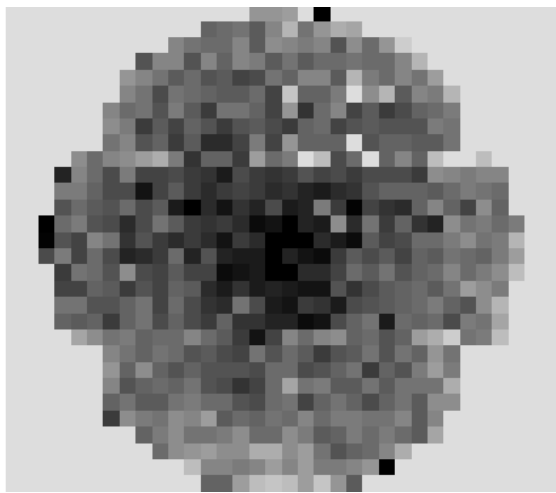
It is believed that these event files offer several improvements over previous versions (e.g. those of Lumb et al. (2002), themselves improvements on previously-created versions) for several reasons. Important points are as follows (note that many of the points are particularly important not only as regards the event files, but also the above background maps);

- The event files have been created separately for each combination of instrument, instrument mode and filter. Hence, event files now exist for medium filter and also for pn full-frame-extended mode, neither of which had existed previously.
- As stated in the analysis sections, all data are collected from source-subtracted and high-background filtered fields with no bright sources or diffuse features, which could contaminate the ‘background’, even after source-subtraction.
- The datasets are very long, longer than previously created event files (over a million seconds of clean low-background data exists in each of the thin filter MOS datasets, for example). This allows further improved signal-to-noise.
- The secondary extensions of the files have been removed, and all headers cleaned and corrected. This results in far smaller and more manageable files. It is possible to treat the event files as normal SAS event files; images, spectra and lightcurves can be created via *evselect*, and one can run *ftools* on the files.
- The event files consist of many more shorter exposure observations (rather than a few, long observations), such that the holes left by the source-subtraction are of less importance, and are heavily diluted by data from other observations. Due partly to the different exposure times of the individual observations, no definite flux limit exists above which sources have been removed. However, flux histograms of the detected and thereafter removed sources do show quite a sharp cutoff at $\approx 1 \times 10^{-14}$ erg cm⁻² s⁻¹) (see <http://www.sr.bham.ac.uk/xmm3/BGproducts.html>).
- The exposure times are believed to be accurate, and include losses due to downtime.

5.1 Event files: usage and caveats

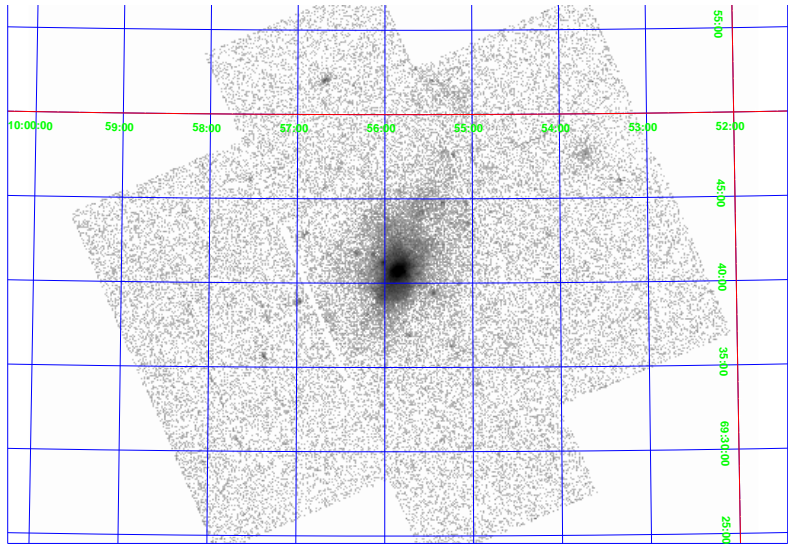
The eight event files are named in a similar manner to the background maps. *E1_ft0000_M1.fits* is a MOS1 full-frame, thin filter event file. PN and M2 are for the pn and MOS2 instruments, an *e* denotes extended full-frame mode, and an *m*, medium filter.

As regards using the event files for background analysis, it is strongly suggested consulting Lumb et al. (2002). Because of the above improvements, a number of the caveats are now not relevant as regards the present files. Many however, are still valid.

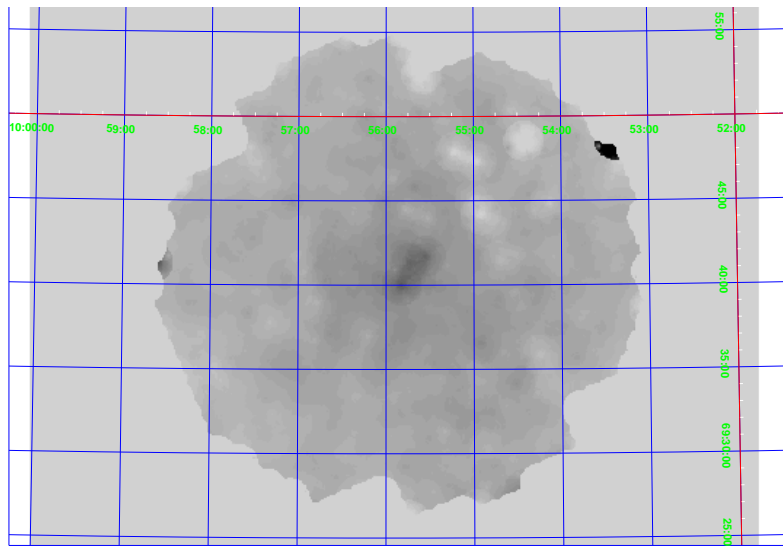


BG image (DETX/Y; 1')

&



User's source image (Sky; ?")



Rebinbed & sky-projected BG image (Sky; ?")

Figure 4: Usage of BGrebinimage2SKY to rebin and sky-project a given low-resolution DETX/Y background map (top left) to the spatial binning and sky position of a user-created high-resolution sky image (top right). The resultant high-resolution sky background image is shown at the bottom. (Note that a poor quality, immature version of a background image has been used to show more clearly the rebinning and reprojecting.)

- The user should take care in extracting background from an appropriate region. This can be done in detector coordinates, though the background event files can be *skycast* onto the sky position of the user's field (see <http://www.sr.bham.ac.uk/xmm3/> - alternatively use the XMM-SAS task *attcalc*).
- Remnant low-level flares will remain in the event files. It is known, for instance, that at low energies, the proton flares turn on more slowly, but earlier than the main flare. The user is able to apply further, more stringent flare-screening to the event files than that performed in their formation, but note that the lowest level proton fluxes may be spectrally variable, so that no complete subtraction may be possible.
- Although point sources have been removed, examination of images created from the datasets does reveal fluctuations in intensity. Over scales of arcminutes appropriate to extended sources, it is not expected to be a significant problem, and indeed representative of unresolved background. If a user however, should try to extract spectra from regions comparable to the PSF scale, care should be taken, and a manual inspection may be necessary to guard against a local excess or deficit of counts arising from the point source extraction procedures. In some of the present cases, it is true that, as many of the observations were pointed such that the target source was at the centre of the detector, a deficit in counts is seen at this position.
- Many defects are seen at the lowest energies (below 0.3 keV), and the calibration of the EPIC response at these energies is not so well understood as it is at higher energies. Care should be taken when performing analysis below around 0.25 keV.

6 Final remarks

At this time of writing, there has been only scant experience gained in using either the maps, the event files or the related software. Any feedback on using the datasets would be very useful and is most welcome (please email any comments to amr@star.sr.bham.ac.uk).

It is hoped that further releases of the datasets, created using larger numbers of pointed observations, and perhaps using further modes and filters, will be made available in the future. This will be announced in the usual manner and via the URL <http://www.sr.bham.ac.uk/xmm3/>.

AMR wishes to acknowledge Trevor Ponman & Laurence Jones (Birmingham) for very useful discussions during this work, and Mike Denby (Leicester, SSC) for making many datasets available.

References

- [1] Arnaud M., et al., 2001, 'Measuring cluster temperature profiles with XMM-Newton', *A&A*, 365, L80
- [2] de Luca A., Molendi S., 2002, 'Studying the cosmic X-ray background with XMM-Newton', *astro-ph/0202480*
- [3] Ghizzardi S., 2000, 'Analysis of the MOS instrumental background', EPIC-MCT-TN-003
- [4] Lumb D., 2002, 'EPIC background files', <http://xmm.vilspa.esa.es/docs/documents/CAL-TN-0016-2-0.ps.gz>
- [5] Lumb D., Warwick R.S., Page M., de Luca A., 2002, 'X-ray background measurements with XMM-Newton EPIC', *A&A*, 389, 93
- [6] Marty P.B., Kneib J.-P., Sadat R., Ebeling H., Smail I., 2002, 'Data analysis methods for XMM-Newton observations of extended sources.', *astro-ph/02009270*
- [7] Molendi S., 2001, 'Spatially Resolved Spectroscopy with EPIC', <http://xmm.vilspa.esa.es/sas/workshops/estec2001/smolendi/smolendi-viewgraphs/slide.ps.gz>
- [8] Pratt G., et al., 2001, 'XMM-Newton observations of galaxy clusters: the radial temperature profile of A2163', *astro-ph/0105431*
- [9] Strüder L., et al., 2001 'The EPIC on XMM-Newton: the pn-CCD camera', *A&A*, 365, L18
- [10] Turner M., et al., 2001 'The EPIC on XMM-Newton: the MOS-CCD camera', *A&A*, 365, L27

Appendix: The XMM-Newton X-ray Background – Additional notes

Several members of the community have been analysing various aspects of the XMM-Newton background, and many of these are described in Marty (2002), Lumb (2002) & Lumb et al. (2002). The reader is strongly encouraged to study Lumb et al. (2002).

A number of datasets have also been analysed, collected and merged together. Two sets of data are particularly relevant as regards the present analysis:

Background datasets have been produced by Dave Lumb (Lumb 2002, Lumb et al. 2002) for the three EPIC instruments by source-subtracting and co-adding a few long observations. These event files can be obtained from <http://xmm.vilspa.esa.es/ccf/epic/#background>, along with very useful explanatory notes (<http://xmm.vilspa.esa.es/docs/documents/CAL-TN-0016-2-0.ps.gz>)

Event lists combining several CLOSED observations have been created by Phillippe Marty, and these have also proven very useful in the analysis and background-subtraction of extended objects (see Sect.3.2). These data can be obtained from <ftp://www-station.ias.u-psud.fr/pub/epic/Closed>

In addition, several novel methods have been used to analyse very extended and diffuse X-ray sources, where the extraction of the background is difficult. Many of these are described in Marty et al. 2002. Of special interest is the work of Arnaud et al. (2001), de Luca & Molendi (2002), Ghizzardi et al. (2000), Molendi (2001), Pratt et al. (2001) and many others.